Journal of Cardiology 75 (2020) 400–409

Contents lists available at ScienceDirect

Journal of Cardiology

journal homepage: www.elsevier.com/locate/jjcc

Original article

Clinical usefulness of quantification of myocardial blood flow and flow reserve using CZT-SPECT for detecting coronary artery disease in patients with normal stress perfusion imaging

Shinya Shiraishi (MD, PhD)[a,*], Noriko Tsuda (MD, PhD)[a], Fumi Sakamoto (MD, PhD)[a], Kouji Ogasawara (MD)[a], Seiji Tomiguchi (MD, PhD)[b], Kenichi Tsujita (MD, PhD, FJCC)[c], Yasuyuki Yamashita (MD, PhD)[a]

[a] Department of Diagnostic Radiology, Graduate School of Life Sciences, Kumamoto University, Kumamoto, Japan
[b] Department of Diagnostic Medical Imaging, School of Health Faculty of Life Sciences, Kumamoto University, Kumamoto, Japan
[c] Department of Cardiovascular Medicine, Graduate School of Life Sciences, Kumamoto University, Kumamoto, Japan

ARTICLE INFO

Article history:
Received 28 May 2019
Received in revised form 18 August 2019
Accepted 3 September 2019
Available online 18 November 2019

Keywords:
Myocardial perfusion reserve
Dynamic single-photon emission computed tomography
Cardiac cadmium zinc telluride gamma camera
Coronary artery disease
Normal stress myocardial perfusion

ABSTRACT

Background: Relative myocardial perfusion imaging can misdiagnose "balanced" ischemia caused by coronary artery disease (CAD). We assessed the feasibility of myocardial blood flow (MBF) and myocardial perfusion reserve (MPR) using dynamic single-photon emission computed tomography (SPECT) with a cadmium-zinc-telluride (CZT) camera for estimating underlying CAD in patients with normal stress myocardial perfusion SPECT (MPS).

Methods: 125 patients with normal stress MPS (summed stress score ≤3) were enrolled. All patients underwent coronary angiography (CAG) and stress/rest ^{201}Tl dynamic SPECT for MBF and MPR calculation. The diagnostic accuracy of both these quantitative values and other clinical risk factors for predicting occult CAD were validated by CAG.

Results: MPR was 2.85 in patients with no CAD, 2.47 with 1-, 1.98 with 2-, and 1.76 with 3-vessel CAD. The patient's age, morbidity of diabetes mellitus (DM), chronic kidney disease (CKD), stress MBF, and MPR were significantly associated with the presence of CAD (age, $p = 0.02$; DM, $p = 0.005$; CKD, $p = 0.005$; creatinine level, $p = 0.012$, stress MBF, $p = 0.019$, and MPR, $p < 0.001$). Independent predictors in the multivariate regression analysis were as follows: DM, $p = 0.011$, CKD, $p = 0.028$, and MPR, $p < 0.001$. The combined index was calculated from three independent predictors. Area under the receiver operating characteristic curve was 0.75 for MPR and 0.81 for the combined index. To identify CAD, sensitivity, and specificity for MPR were 77% and 66%, and for the combined index they were 79% and 66%, respectively.

Conclusion: Quantification of MPR and MBF using dynamic SPECT with a CZT camera can be useful to identify balanced ischemia caused by occult CAD in patients with normal stress MPS findings.

Introduction

Radionuclide myocardial perfusion imaging (MPI) allows the visualization of radiopharmaceuticals distributed throughout the myocardium in proportion to the myocardial blood flow (MBF) and this facilitates the determination of the relative blood flow in various regions of the heart. Myocardial perfusion single-photon emission computed tomography (MPS) is a widely used non-invasive technique to evaluate ischemia and to stratify risk factors in patients with known or suspected coronary artery disease (CAD) [1–3].

However, crucial limitations with respect to visual or semi-quantitative assessment of regional myocardial perfusion defects can result in the underestimation or misdiagnosis of "balanced" ischemia. In other words, in patients with a balanced multi-vessel CAD or microcirculatory disorders a global reduction in myocardial perfusion can be completely overlooked when assessment is based solely on the relative radiotracer uptake.

* Corresponding author at: Department of Diagnostic Radiology, Faculty of Life Sciences, Kumamoto University, 1-1-1 Honjo, Chuo-ku, Kumamoto, 860-8556, Japan.
E-mail address: shiraish@kumamoto-u.ac.jp (S. Shiraishi).

https://doi.org/10.1016/j.jjcc.2019.09.006
0914-5087/

This eventuality can be surmounted by the quantification of MBF or myocardial perfusion reserve (MPR) using a tracer kinetic method for positron emission tomography (PET) [4–7]. Stress- and rest flow measurements provide an integrated measure of the ischemic burden due to microvascular or macrovascular disease [8] and they are superior to the assessment of relative perfusion alone for detecting the initial stages of coronary atherosclerosis, stratification of risks for cardiac events, and predicting prognosis in patients with or without conventional cardiac risks [9–15]. However, since the installation of a PET tracer production system involves high costs, this technology is not yet readily available in many areas around the world. Also, measuring MBF with standard single-photon emission computed tomography (SPECT) cameras is difficult because SPECT perfusion quantitation is hampered by the difficulty of performing dynamic acquisitions.

Dedicated ultra-fast cardiac cameras using cadmium zinc telluride (CZT) have greatly improved sensitivity and they do not require to be rotated around the patient. The detectors facilitate tomographic dynamic acquisition and offer the theoretical possibility of investigating radiotracer kinetics in vivo [3,16–18]. However, there is no published report that evaluates the detection of balanced ischemia due to multi-vessel CAD limited to patients with normal stress MPS, that is, summed stress score (SSS) $\leq$3, nor even in a PET evaluation.

This study attempted to evaluate the usefulness of the quantification of the absolute MBF and MPR in a routine clinical setting using ^{201}Tl dynamic SPECT using a CZT camera. Diagnostic performance of the quantitative indicators to evaluate significant CAD was limited to patients with normal stress MPS.

Materials and methods

Study design and subjects

This study was approved by our Institutional Ethics Committee. All study procedures were in accordance with the Statement of Human and Animal Rights. Prior informed consent for inclusion in the study was obtained from all patients or their legal representatives.

Between April 2013 and December 2018, 1008 patients underwent both pharmacologic stress and at-rest dynamic SPECT evaluation with a cardiac CZT camera at our hospital. The exclusion criteria were as follows: (1) abnormal MPS results ($4 \leq$ SSS); (2) without coronary angiography (CAG) within 90 days of the SPECT studies; (3) coronary artery bypass grafting (CABG); (4) non-ischemic cardiomyopathy; (5) myocarditis; (6) cardiac amyloidosis; and (7) severe valvular heart disease. We excluded 867 patients based on the exclusion criteria (abnormal MPS, n = 603; without CAG within 90 days of the SPECT studies, n = 259; history of CABG, n = 3; non-ischemic cardiomyopathy, n = 1; and myocarditis, n = 1). Furthermore, 16 patients were excluded because the dynamic image was not suitable for analysis for technical reasons or because the patient moved during the dynamic scan. Finally, we enrolled 125 patients (mean age 74.8 $\pm$ 7.7 years; 72 males) with both normal MPS results (SSS $\leq$ 3) and who had CAG within 90 days of the SPECT studies. Although these cases were the results of normal MPS, the reasons for doing CAG were as follows: Post percutaneous coronary intervention (n = 60), cause search of anginal pain (n = 22), CAD suspected by coronary CT angiography (CCTA) (n = 15), cause search of heart failure (n = 13), before large artery treatment (n = 7), severe coronary calcification (n = 5), and ST depression (n = 3) (Fig. 1).

For each patient, the presence of clinical risk factors of CAD was noted. The following categories were evaluated: male gender, advanced age, body mass index (BMI), hypertension (defined as a blood pressure 140/90 mmHg or the use of anti-hypertensive medication), dyslipidemia [based on low-density lipoprotein cholesterol (LDL-C)-, high-density lipoprotein cholesterol (HDL-C)-, and triglyceride (TG) level or relevant medication], diabetes mellitus (DM) [revealed by the hemoglobin A1c (HbA1c) level or medication], chronic kidney disease (CKD) [based on the creatinine level and estimated glomerular filtration rate (eGFR)], previous myocardial infarction (MI), a smoking history (Brinkman index), anemia (revealed by the hemoglobin level),cardiac dysfunction [based on the brain natriuretic peptide (BNP) level], and left ventricular ejection fraction (LVEF).

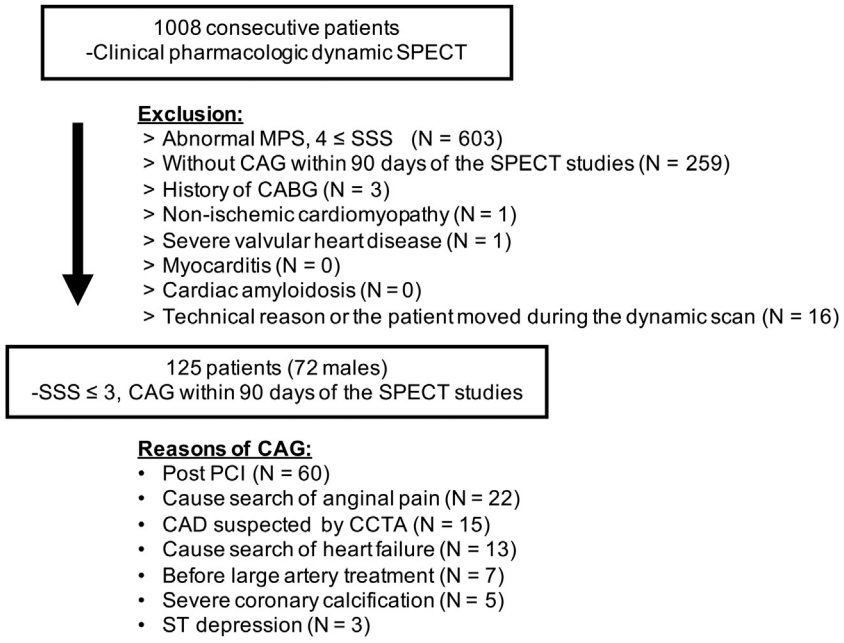

Fig. 1. Study design.
SPECT, single photon emission computed tomography; SSS, summed stress score; CAG, coronary angiography; CABG, coronary artery bypass grafting; PCI, percutaneous coronary intervention; CAD, coronary artery disease; CCTA; coronary computed tomography angiography.

SPECT imaging

MPS was performed using a CZT camera (Discovery NM530c, GE Healthcare, Chicago, IL, USA). Imaging was performed with the patient in the supine position with the arms placed over the head. For MPS stress tests, pharmacologic vasodilator stress was induced by intravenously injecting all patients with adenosine (0.12 mg/kg/min for 6 min). At peak stress, a half dose (50–60 MBq) of the ^{201}Tl chloride was injected into the right arm. The tracer was delivered intravenously as a bolus, followed by a 40 ml saline flush over 20 s. Dynamic imaging was performed under a 6-minute acquisition protocol in list mode. Three-dimensional (3D) axial volumes ($70 \times 70 \times 50$ voxels, $4 \times 4 \times 4$ mm) were reconstructed from the acquired raw data using maximum *a posteriori*-expectation maximization. This generated 72 3D volumes integrating 5-sec time frames in 360 s. Routine gated stress images were acquired after dynamic imaging. Routine gated at-rest images were obtained 3 h after the administration. For at-rest MPS tests, 30-sec pre-scanning was performed to obtain the baseline images. The half dose of the radiotracer was injected in a continuous fashion; sequential dynamic images were recorded in the same manner as the stress imaging. At-rest analysis was performed by subtracting the baseline pre-scan images from the dynamic scans (Fig. 2).

Images were reformatted using Lister software on a Xeleris workstation (GE Healthcare) and reconstructed with a dedicated maximum penalized likelihood expectation maximization iterative algorithm (Myovation for Alcyon, GE Healthcare). For left ventricular function analysis, quantitative gated SPECT software (Cedar-Sinai, Los Angeles, CA, USA) [19] was used.

SPECT images and quantitative analysis

Dynamic images in DICOM format were transferred to a workstation by a MPR analysis tool (Cardiac FPEF) included in the software package called AZE VirtualPlace Hayabusa version 6.1 (AZE, Ltd. Tokyo, Japan). The input function was typically obtained from the results of left ventricular first-pass blood pool analysis. Global segmentation of the left ventricle and determination of the blood pool region was performed automatically. After the reconstruction process, the automatically drawn volume of interest (VOI) was shown on the reframed volume and aligned with the global volume. The VOI-related time-activity curve (TAC) was extracted by averaging the signal intensity in the VOI for each time frame. The number of counts obtained was normalized to the VOI size (mm^3) and the frame duration. The TAC was fitted to a kinetic model using a weighted linear least-squares method to estimate the radiotracer exchange rate and the spill-over coefficients.

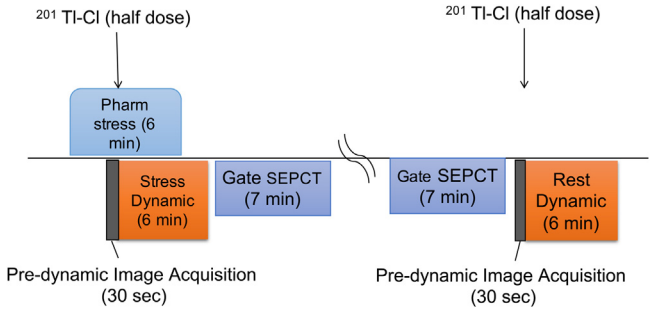

Fig. 2. Single photon emission computed tomography (SPECT) protocol.
Adenosine is infused intravenously and symptoms, blood pressure, and electrocardiogram are monitored. After pre-dynamic image acquisition (30 s), a half dose (50–60 MBq) of ^{201}Tl- chloride is injected into the right arm. The tracer ss delivered intravenously as a bolus, followed by a 40 ml saline flush over 20 s. Dynamic SPECT images are acquired for 6 min and conventional gated SPECT is performed for 7 min. At-rest images are acquired 3 h later, conventional gated SPECT is performed for 7 min. Subsequently, after pre-dynamic image acquisition (30 s), a half dose of ^{201}Tl is injected intravenously and dynamic SPECT images are acquired in the same manner as in stress imaging. At-rest analysis is performed by subtracting the baseline pre-scan image from the dynamic scans.

Global TAC was fitted to the single tissue compartment kinetic model with input functions derived from factor analysis. K1 values were calculated on stress- and at-rest images. Global MBF was derived from the corresponding K1 values using the Renkin-Crone equation for ^{201}Tl [20,21]. MBF value was obtained from the K1 value and corrected for the first-pass extraction fraction (EF) and hematocrit (Hct) using the equation MBF = K1*/EF, where EF = 1-$0.57^{*}e^{-1.02/MBF}$ and K1* = K1/(1-Hct) [22,23]. MPR was then computed as a ratio of the stress to rest MBF values (MPR = stress MBF/rest MBF).

Relative myocardial perfusion was also evaluated. Evaluation was done using a representative system with the assistance of two experienced nuclear medicine physicians. Images were assessed by 17-segment visual interpretation using a 5-point score and SSS, summed rest score, and summed difference score values were calculated. We derived the transient ischemic dilation (TID) ratio from non-gated acquisitions.

Coronary angiography

Patients without intervening coronary events or interventional procedures underwent invasive CAG within 90 days of the dynamic-SPECT evaluation. Cine-angiograms of the coronary arteries were obtained in multiple projections using a standard technique. The angiographic criterion used to define the presence of significant CAD was determined stenosis $\geq$50% in the left main artery, $\geq$70% and/or fractional flow reserve (FFR) $\leq$0.8 in the left anterior descending-, left circumflex-, or right coronary artery and the main branching vessels.

Statistical analysis

Continuous variables were presented as the mean (standard deviation). Categorical variables are the number of patients followed by the percentage in parentheses.

To evaluate the independent predictors of diseased CAD, continuous variables were compared in two groups (non-CAD group vs. 1-, 2-, or 3-vessel CAD group) with the Mann-Whitney *U* test. Categorical variables were compared using the chi-square test. Multivariate forward stepwise regression analysis was performed to evaluate the predictive ability of vessels diseased with CAD. The optimal cut-off points of the significant predictive indicator were obtained through receiver-operating characteristic (ROC) analysis. Lower cut-off values were selected in the range where sensitivity did not fall below 90%, upper cut-off values were selected where specificity did not fall below 90%, and intermediate values were selected at the peak Youden index. Diagnostic accuracy was evaluated by calculating the sensitivity, specificity, positive and negative predictive value (PPV and NPV). Values of p less than 0.05 were considered statistically significant. All statistical analyses were performed using SPSS (version 24.0.0, SPSS Inc., Chicago, IL, USA).

Results

Data for all 125 enrolled patients are presented. A total of 47 (37.6%) patients showed no evidence of CAD, 40 (32.0%) had 1-, 24 (19.2%) 2-, and 14 (11.2%) had 3-vessel CAD. The mean MPR was 2.85 in patients without CAD, 2.47 in the presence of 1-, 1.98 in 2-, and 1,76 in 3-vessel CAD. The stress MFR was 1.62 ml/g/min in patients without CAD, 1.54 in the presence of 1-, 1.27 in 2-, and

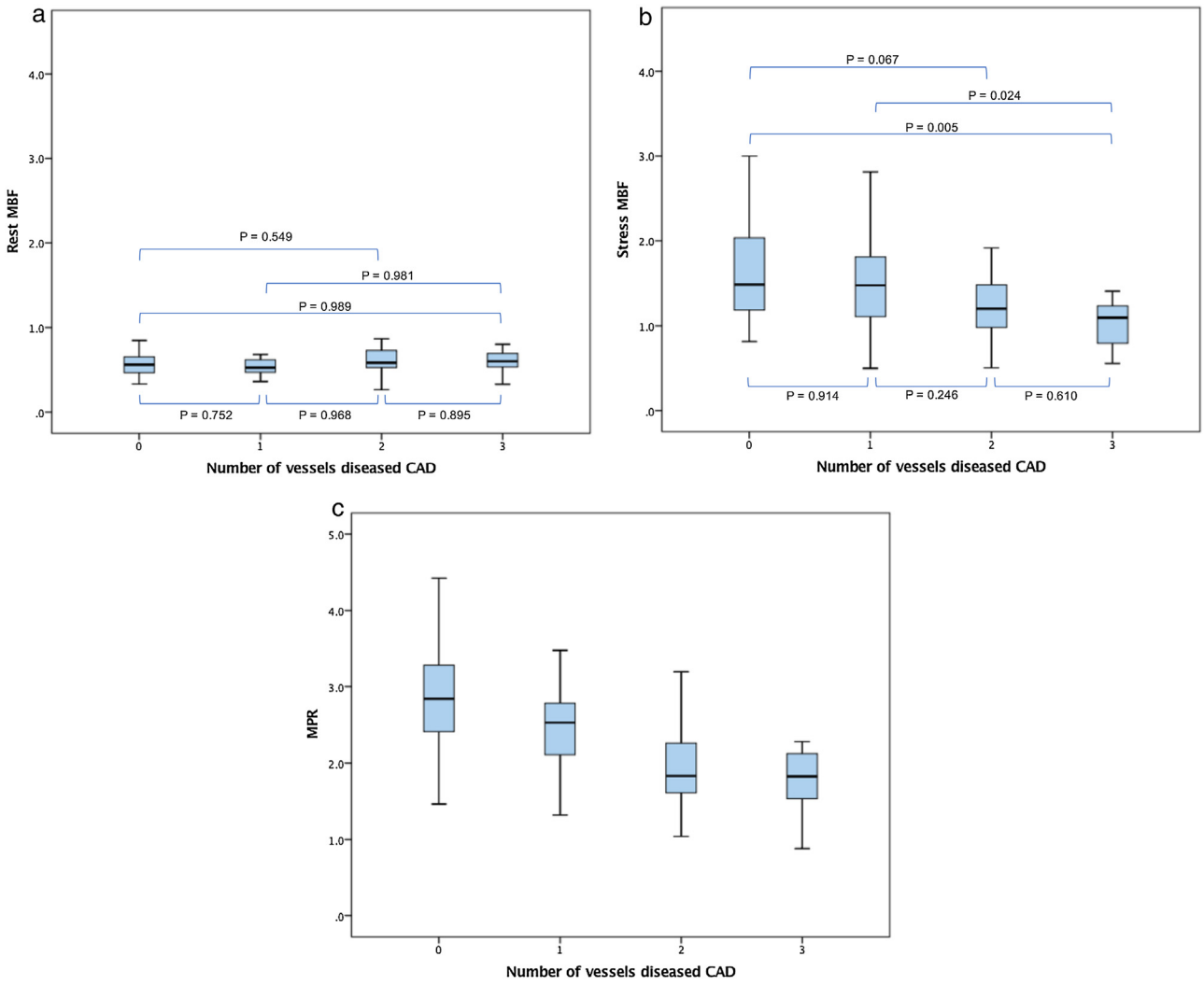

Fig. 3. (**a**) At-rest myocardial blood flow (MBF), (**b**) Stress MBF, (**c**) myocardial perfusion reserve (MPR) vs. extent of angiographic disease.

1.04 in 3-vessel CAD. The at-rest MFR was 0.58 ml/g/min in patients with no coronary vessel disease, 0.63 in the presence of 1-, 0.66 in 2-, and 0.60 in 3-vessel CAD (Fig. 3).

The characteristics of two patient groups with and without CAD are presented in Table 1. Age was significantly higher in patients with CAD than in patients without CAD (non-CAD vs. CAD: 72.7 ± 8.2 vs. 76.0 ± 7.2, $p = 0.02$). The prevalence of DM was significantly higher in patients with CAD (non-CAD vs. CAD: 28% vs. 53%, $p = 0.005$). The prevalence of CKD was significantly higher in patients with CAD (non-CAD vs. CAD: 45% vs. 71%, $p = 0.005$). The stress MBF was significantly lower in the presence of CAD (non-CAD vs. CAD: 1.62 ± 0.55 vs. 1.54 ± 0.66 mL/g/min, $p = 0.019$). MPR was significantly lower in the presence of CAD (non-CAD vs. CAD: 2.85 ± 0.73 vs. 2.47 ± 0.53, $p < 0.001$). Independent predictor variables of the patients with CAD that remained in the multivariate regression analysis were as follows: DM [β = 3.35 (1.51–9.57), $p = 0.011$], CKD [β = 2.76 (1.03–6.14), $p = 0.028$], and MPR [β = 0.23 (0.12–0.48), $p < 0.001$] (Table 2). Our formula for calculating the combined index from three independent predictors was: −0.04 -1.43 × MPR + 1.21 × DM (positive, 1; negative, 0) + 1.01 × CKD (positive, 1; negative, 0). ROC analysis of the MPR and the combined index was performed to obtain the rea under the receiver operating characteristic curve and determination of cut-off points exhibiting difference between the following groups of patients with CAD (for the MPR, non-CAD vs. CAD, AUC = 0.75, cut-off point ≤2.66, $p < 0.001$; and for the combined index, non- CAD vs. CAD, AUC = 0.81, cut-off point ≤ −0.10). For MPR, sensitivity, specificity, PPV, NPV, and accuracy were 77%, 66%, 79%, 63%, and for combined index, were 79%, 66%, 79%, and 66%, non- CAD group vs. CAD group (Table 2).

Patients were classified by using the cut-off value of 3 independent predictors of CAD patients with normal myocardial perfusion SPECT (MPR, presence of CKD, and presence of DM). The total number of patients with and without CAD and positive predictive values are shown in Fig. 4 as is the number and percentage of patients with CAD in each category.

Discussion

To our knowledge, this study is the first evaluation with respect to the feasibility of quantifying the MBF and MPR using CZT-SPECT with ^{201}Tl to detect occult CAD considered to be the cause of balanced ischemia. Patients enrolled were limited to cases within a normal range of MPS (SSS ≤ 3). The preliminary evidence obtained suggests stress MBF and MPR are significant independent predictors of CAD in parameters. Representative cases are presented in Fig. 5. There was a significant stepwise reduction in stress MBF and MPR as the extent of obstructive CAD increased. The addition of combined indexes including MPR, DM, and CKD further contributed. These results add new and important

Table 1
Patient characteristics and single-photon emission computed tomography findings between the groups of patients with 0- and 1–3 vessel coronary artery diseases.

	Non-CAD	1-, 2-, or 3-vessel CAD	*p*	
	n = 47	n = 78	Univariate analysis	multivariate analysis
Age	72.7 ± 8.2	76.0 ± 7.2	0.02	0.454
Gender /male	22 (47%)	50 (64%)	0.059	
BMI	23.2 ± 4.1	23.1 ± 3.2	0.856	
Hypertension	34 (72 %)	64 (82 %)	0.223	
Dyslipidemia	29 (62 %)	54 (69 %)	0.392	
DM	13 (28 %)	41 (53 %)	0.005	0.003
CKD	21 (45%)	53 (71 %)	0.005	0.037
Previous MI	6 (13 %)	8 (20 %)	0.773	
Brinkman index	264 ± 430	559 ± 777	0.476	
Hemoglobin	12.6 ± 2.0	11.9 ± 1.6	0.065	
TG	117 ± 59	129 ± 66	0.303	
HDL-Cholesterol	53 ± 17	50 ± 13	0.287	
LDL-Cholesterol	94 ± 30	87 ± 31	0.207	
Hemoglobin A1c	6.1 ± 0.8	6.5 ± 1.2	0.117	
Creatinine	1.28 ± 1.27	2.02 ± 2.95	0.053	
Estimated GFR	56 ± 24	49 ± 25	0.119	
BNP	185 ± 396	148 ± 296	0.553	
LVEF	60 ± 17	61 ± 12	0.952	
TID	1.13 ± 0.14	1.15 ± 0.11	0.409	
Stress MBF	1.62 ± 0.55	1.37 ± 0.58	0.019	0.826
Rest MBF	0.58 ± 0.18	0.63 ± 0.25	0.213	
MPR	2.85 ± 0.73	2.19 ± 0.59	<0.001	<0.001

BMI, body mass index; CAD, coronary artery disease; DM, diabetes mellitus; CKD, chronic kidney disease; HDL-C, high-density lipoprotein cholesterol; LDL-C, low-density lipoprotein cholesterol; MI, myocardial infarction; TG, triglyceride; GFR, glomerular filtration rate; BNP, brain natriuretic peptide; LVEF, left ventricular ejection fraction; TID, transient ischemic dilatation; MBF, myocardial blood flow; MPR, myocardial perfusion reserve.

Table 2
Diagnostic accuracy of MPR and combined index in the prediction of coronary artery disease at different thresholds.

Predictor	Threshold Parameter	Cut-off value	TP	FP	FN	TN	Sensitivity (%)	Specificity (%)	PPV (%)	NPV (%)	Youden index
MPR	Sensitivity 90%	2.95	70	25	8	22	90	47	74	73	0.366
	Peak Youden	2.66	60	16	18	31	77	66	79	63	0.429
	Specificity 90%	1.8	24	5	54	42	31	89	83	44	0.201
Combined index	Sensitivity 90%	0.43	70	23	8	24	90	51	75	75	0.408
	Peak Youden	0.52	62	16	16	31	79	66	79	66	0.454
	Specificity 90%	0.75	41	5	37	42	53	89	89	53	0.419

MPR, myocardial perfusion reserve; FN, false-negative; FP, false-positive; NPV, negative predictive value; PPV, positive predictive value; TN, true-negative; TP, true-positive.

information to the findings obtained with conventional SPECT studies on patients with known or suspected CAD.

^{201}Tl-Cl is a widely used myocardial perfusion tracer. However, the radiation exposure is greater with ^{201}Tl than ^{99m}Tc tracers; the average radiation exposure per study reported by the International Commission on Radiological Protection was 15.5 mSv [24]. Therefore, we used only half of the ^{201}Tl dose that is usually administered for at-rest and stress tests. Even with low radiotracer doses, the high sensitivity and high resolution of the CZT camera yields high-quality images. ^{201}Tl is considered ideal for the quantification of absolute MBF because of its high first-pass extraction fraction and large distribution volume [21,22]. Because the results of ^{99m}Tc tracers showed the expected reduction in the measured K1 values at a higher blood flow [25], ^{201}Tl for the quantitative assessment was selected for this study.

Balanced myocardial ischemia due to CAD, particularly multivessel CAD or microvascular dysfunction in patients with suspected ischemic heart disease poses a diagnostic dilemma for the nuclear medicine physician. Injection of radiotracers in patients with relatively balanced ischemia may result in a homogenous distribution in the myocardium and lead to an underestimation of the severity of ischemia and return false-normal findings. Murthy et al. [9] showed that a decreased flow reserve on PET imaging was a powerful independent predictor of cardiac mortality, possibly because MPR and stress MBF measurements are deeply related to disease severity. Furthermore, quantitative estimates of MPR obtained can be useful in identifying balanced ischemia. Ziadi et al. concluded the integration of quantitative flow analysis could help to improve the detection of 3-vessel CAD to relative MPI. In 88% of their patients with severe 3-vessel CAD, MPR was globally reduced (<2) [26]. Fiechter et al. evaluated the added diagnostic value of MFR on ^{13}N-ammonia PET/CT to predict angiographic CAD and showed that 33% of patients with normal MPI findings were correctly reclassified as having abnormal findings when MFR information was added [27]. Naya et al. reported the largest angiographic study of the interaction between quantitative CFR and extent and severity of CAD. They found that normal CFR has a high negative predictive value (97%) for excluding high-risk CAD on angiography [28]. However, considering the widespread clinical use of PET due to higher costs and more complicated procedures, MPS remains the clinical standard for assessing ischemia. Advances in nuclear cardiology due to the dedicated ultra-fast cardiac cameras has provided high-quality, high-resolution, and high-diagnostic myocardial images [29,30] and facilitated tomographic dynamic acquisition with the theoretical possibility of investigating radiotracer kinetics in vivo. Use of CZT cameras enables estimation of MPR [31]. Clinical studies found a good correlation between the global MPR and the severity

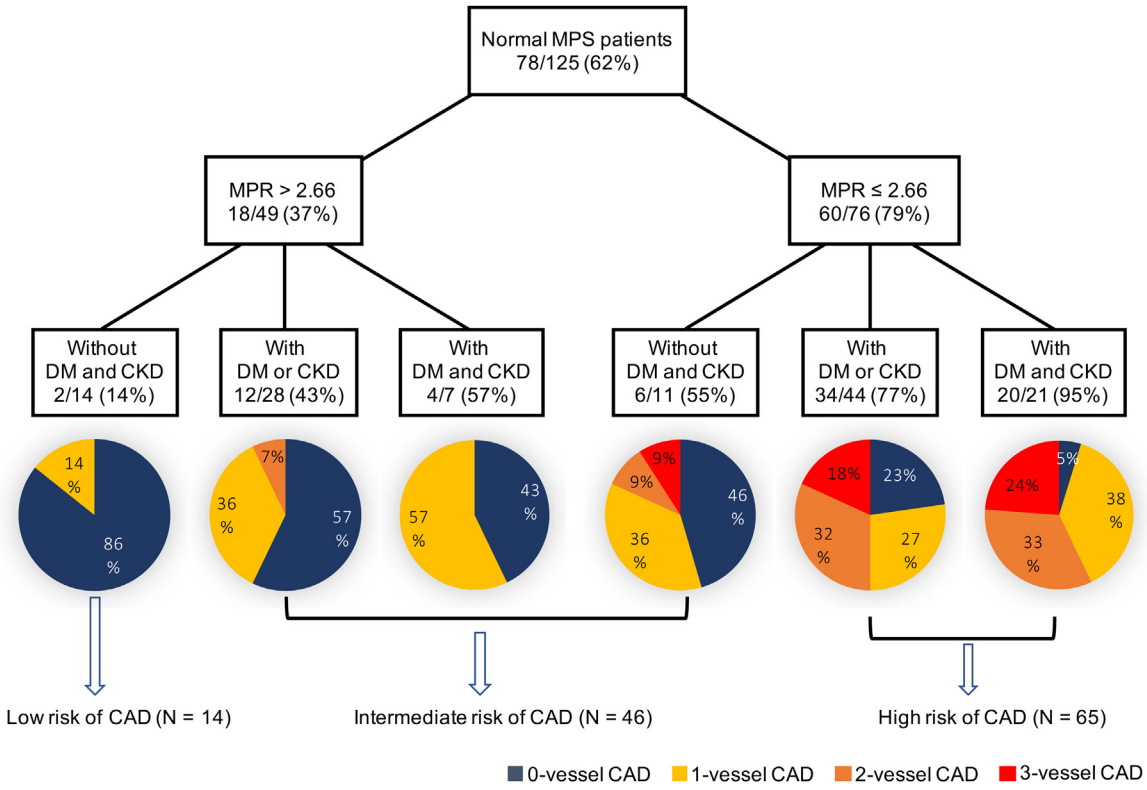

Fig. 4. Decision tree using independent predictors of coronary artery disease (CAD), diabetes mellitus (DM), and chronic kidney disease (CKD).
Using the cut-off value of 2.66 of the myocardial perfusion reserve (MPR) and with or without DM and CKD, patients with normal myocardial perfusion SEPCT (MPS) were classified into groups. Percentages in boxes represent the proportion of patients with CAD in each group. Percentages in circle graphs is the proportion of extent of angiographic disease within each group.

of CAD, expressed as the stress total perfusion deficit [16]. The global and regional MPR was also predictive of the extent of CAD [32] and agreed with the FFR measurements on invasive angiographs [3]. We previously reported that MPR using a CZT camera can identify balanced ischemia in patients with a left main or 3-vessel disease [17]. However, no studies have been reported on PET evaluations to detect the unnoticed CAD by quantifying the MBF in patients limited to those with normal MPS findings.

As to the 125 patients with normal MPS findings who underwent CAG, age, DM, and CKD, stress MBF, and MPR were significant independent predictors of the occult CAD. Subsequent multivariate forward stepwise regression analysis indicated that MPR and presence of DM and CKD were independent predictors and a formula to calculate the combined index from these predictors was established. Both the combined index and MPR were documented as accurate indicators for diagnosing occult CAD at an AUC of 0.81 and 0.75, respectively. As shown in Table 2 and Fig. 4, when evaluated even with MPR alone, the sensitivity for a diagnosis of CAD was 77% with a cut-off value of <2.66 and that of 2- or 3- vessel CAD was 95%. Remarkably, detection of CAD proved impossible in 77% of the patients diagnosed as being within the normal range by the conventional examination, despite the fact that they had those lesions. In addition, PPV is not as high as 79%, because MPR decline is not always restricted to epicardial CAD. In CAD, epicardial coronary artery lesions accompanied by diffusely expanded arteriosclerosis without localized stenosis and micro-circulation disturbance are also considered as relevant factors. Whereas, it has been reported that in clinical examinations, anemia [33,34], CKD [33], DM [35,36], hypo HDL-cholesterolemia [37], reduction of LVEF, increase of BNP [38–40], etc. affect microcirculation disorders of coronary vessels and consequently MPR and CFR can be decreased. These observations indicate MPR is not a specific indicator for the detection of epicardial CAD. Therefore, evaluation of CAD using CCTA is recommended if the MPR value is low in patients with normal MPS. Lacking obvious CAD, MPR reduction suggests a microcirculatory impairment due to some other factors, as well as encourage medical treatment for risk factors. NPV was also not as high as 63% using MPR alone (Table 2).However, in cases limited to multi-vessel CAD, NPV rises to 96%, if MPR is 2.66 or more (Fig. 4). This result might be indicating that if the diagnosis by conventional MPS is normal and the MPR value is also normal, the possibility of multi-vessel CAD is considerably low.Fig. 4 shows the effective utilization of MPS when quantification of MBF is applied.

Table 3 summarizes clinical risk factors, MBF quantitative values, and CAD in a high- and a low-risk subgroup. In cases with MPR > 2.66 and without DM and CKD, because the frequency with CAD is as low as 14%, moreover all CAD are 1-vessel disease, and the average value of other CAD risk factors is also in the normal range, optimal medical therapy is considered to be sufficient. Whereas high-risk subgroup patients with MPR ≤ 2.66 and with DM and/or CKD has CAD at 83% and since the decrease of LVEF and the BNP rise are seen as a tendency of heart failure, optical medical therapy alone is insufficient, and it is also necessary to consider precise examinations of CAD through CCTA or CAG.

This study has some limitations. First, in the 47 patients without CAD, values for the MPR (2.85 ± 0.73) in Table 2 were lower than in the PET study reported by Sdringola et al. [41]. The adenosine dose (0.12 mg/kg/min) authorized for use in Japan is lower than the generally-administered dose of 0.14 mg/kg/min and may not have induced the highest hyperemic state. Secondly, because the novel semiconductor dedicated SPECT camera used cannot perform attenuation correction, the presence of attenuation artifacts might have resulted in underestimating the K1 values and MBF due to a

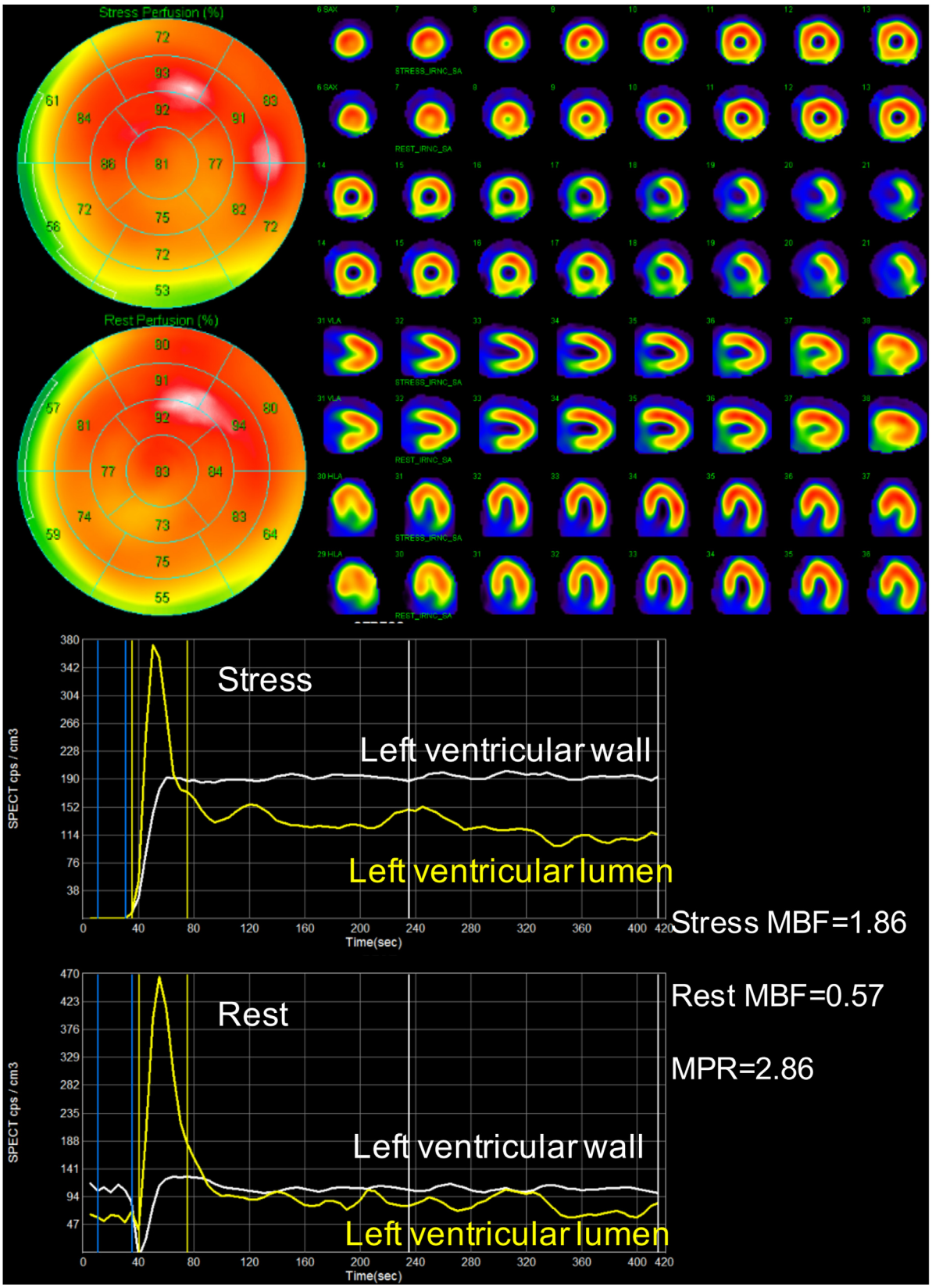

Fig. 5. Representative cases. Upper panels are myocardial perfusion SPECT (MPS) images. Lower panels are time activity curves for quantitative MPS. Yellow lines show the left ventricular blood pool curves as input functions and white lines show the left ventricular myocardium curves as output functions. (A) 74-year-old man without significant stenosis on coronary angiography. (B) Image obtained from a 48- year-old man with 3-vessel stenosis on coronary angiography (left anterior descending artery segment 7, 75%; left circumflex artery segment 11, 75%; segment 13, 75%; right coronary artery segment 3, 75%], chronic kidney disease and diabetes mellitus. Both A and B show a normal range of the summed stress score. However, myocardial perfusion reserve (MPR) and myocardial blood flow (MBF) in case B show low value of 1.72 and 0.91 against 2.86 and 1.86 in case A, respectively.

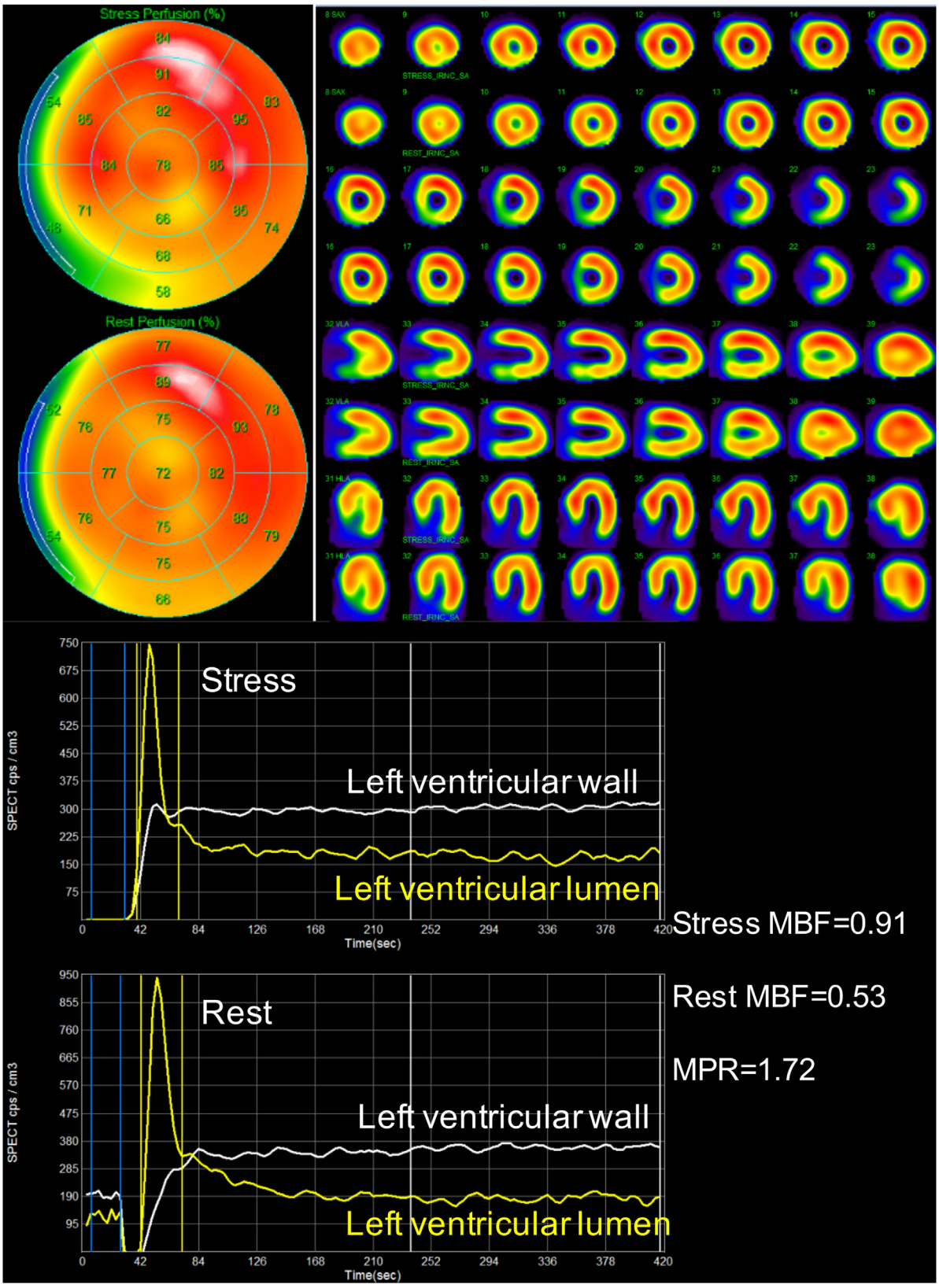

Fig. 5. (*Continued*).

change in the TAC amplitude. Thirdly, regional MPR in the 17 segments was not assessed because, to calculate the MBF in such models, the detected counts were not sufficiently high for drawing a TAC, and a curve based on insufficient counts increases the likelihood of measurement errors. Accurate regional MBF analysis is difficult because attenuation-, spillover-, or motion artifacts vary in different areas. Therefore, using the whole LV rather than regional MPR was the criterion of choice for evaluation

Table 3
Difference between CAD risk groups based on presence of diabetes mellitus or chronic kidney disease and MPR.

	Low-risk group (n = 14)	High-risk group (n = 65)	*p*
Age	68.1 ± 9.7	76.5 ± 6.2	0.007
Gender (male)	7 (50%)	41 (63%)	0.37
BMI	24.3 ± 3.6	23.0 ± 3.4	0.236
Hypertension	10 (71 %)	49 (77 %)	0.667
Dyslipidemia	9 (64 %)	43 (66 %)	0.895
DM	0 (0 %)	35 (54 %)	<0.001
CKD	0 (0%)	51 (78 %)	<0.001
Previous MI	0 (0 %)	8 (11 %)	0.001
Brinkman index	189 ± 314	522 ± 818	0.104
Hemoglobin	13.3 ± 1.4	11.7 ± 1.9	0.004
TG	151 ± 69	123 ± 56	0.104
HDL-C	57 ± 17	50 ± 13	0.093
LDL-C	95 ± 33	85 ± 329	0.283
Hemoglobin A1c	6.1 ± 0.6	6.4 ± 0.8	0.283
Creatinine	0.7 ± 0.1	2.4 ± 3.2	<0.001
Estimated GFR	75 ± 11	44 ± 25	<0.001
BNP	51 ± 77	246 ± 445	0.002
LVEF	66 ± 9	59 ± 15	0.022
TID	1.16 ± 0.09	1.14 ± 0.14	0.49
Stress MBF	2.03 ± 0.51	1.22 ± 0.54	<0.001
Rest MBF	0.63 ± 0.17	0.63 ± 0.27	0.931
MPR	3.28 ± 0.49	1.94 ± 0.41	<0.001
Presence of CAD	2 (14%)	54 (83%)	<0.001
0-vessel CAD	12 (86%)	11 (17%)	<0.001
1-vessel CAD	2 (14%)	21 (32%)	0.125
2-vessel CAD	0 (0%)	20 (31%)	<0.001
3-vessel CAD	0 (0%)	13 (20%)	<0.001

BMI, body mass index; CAD, coronary artery disease; DM, diabetes mellitus; CKD, chronic kidney disease; HDL-C, high-density lipoprotein cholesterol; LDL-C, low-density lipoprotein cholesterol; MI, myocardial infarction; TG, triglyceride; GFR, glomerular filtration rate; BNP, brain natriuretic peptide; LVEF, left ventricular ejection fraction; TID, transient ischemic dilatation; MBF, myocardial blood flow; MPR, myocardial perfusion reserve.

in this study. Fourthly, motion correction was not performed. Efforts are underway in our laboratory to develop appropriate software to address these issues. Lastly, this analysis was applied for quite limited patients and it is uncertain whether this result is able to apply for the diagnosis of CAD patients in general clinical setting. Therefore, we would like to consider a prospective study using the cut-off value derived from this study.

Conclusion

This is the first study to evaluate detectability of CAD by the quantification of absolute myocardial perfusion using a dedicated cardiac CZT camera in limited cases judged to be within the normal range on conventional MPS. The simple quantitative analysis may be useful to identify balanced ischemia caused by latent CAD.

Funding sources

None.

Disclosures

The authors declare that there is no conflict of interest.

Acknowledgments

None.

References

[1] Hendel RC, Berman DS, Di Carli MF, Heidenreich PA, Henkin RE, Pellikka PA, et al. ACCF/ASNC/ACR/AHA/ASE/SCCT/SCMR/SNM 2009 appropriate use criteria for cardiac radionuclide imaging: a report of the American College of Cardiology Foundation Appropriate Use Criteria Task Force, the American Society of Nuclear Cardiology, the American College of Radiology, the American Heart Association, the American Society of Echocardiography, the Society of Cardiovascular Computed Tomography, the Society for Cardiovascular Magnetic Resonance, and the Society of Nuclear Medicine. Circulation 2009;119:e561–87.

[2] Shaw LJ, Hage FG, Berman DS, Hachamovitch R, Iskandrian A. Prognosis in the era of comparative effectiveness research: where is nuclear cardiology now and where should it be? J Nucl Cardiol 2012;19:1026–43.

[3] Miyagawa M, Nishiyama Y, Uetani T, Ogimoto A, Ikeda S, Ishimura H, et al. Estimation of myocardial flow reserve utilizing an ultrafast cardiac SPECT: comparison with coronary angiography, fractional flow reserve, and the SYNTAX score. Int J Cardiol 2017;244:347–53.

[4] Hara T, Michihata T, Yokoi F, Sakamoto S, Masuoka T, Iio M. Quantitative measurement of regional myocardial blood flow in patients with coronary artery disease by intravenous injection of 13N-ammonia in positron emission tomography. Eur J Nucl Med 1990;16:231–5.

[5] Muzik O, Duvernoy C, Beanlands RS, Sawada S, Dayanikli F, Wolfe Jr ER, et al. Assessment of diagnostic performance of quantitative flow measurements in normal subjects and patients with angiographically documented coronary artery disease by means of nitrogen-13 ammonia and positron emission tomography. J Am Coll Cardiol 1998;31:534–40.

[6] Yoshinaga K, Katoh C, Noriyasu K, Iwado Y, Furuyama H, Ito Y, et al. Reduction of coronary flow reserve in areas with and without ischemia on stress perfusion imaging in patients with coronary artery disease: a study using oxygen 15-labeled water PET. J Nucl Cardiol 2003;10:275–83.

[7] Parkash R, deKemp RA, Ruddy TD, Kitsikis A, Hart R, Beauchesne L, et al. Potential utility of rubidium 82 PET quantification in patients with 3-vessel coronary artery disease. J Nucl Cardiol 2004;11:440–9.

[8] Schelbert HR. Anatomy and physiology of coronary blood flow. J Nucl Cardiol 2010;17:545–54.

[9] Murthy VL, Naya M, Foster CR, Hainer J, Gaber M, Di Carli G, et al. Improved cardiac risk assessment with noninvasive measures of coronary flow reserve. Circulation 2011;124:2215–24.

[10] Ziadi MC, Dekemp RA, Williams KA, Guo A, Chow BJ, Renaud JM, et al. Impaired myocardial flow reserve on rubidium-82 positron emission tomography imaging predicts adverse outcomes in patients assessed for myocardial ischemia. J Am Coll Cardiol 2011;58:740–8.

[11] Herzog BA, Husmann L, Valenta I, Gaemperli O, Siegrist PT, Tay FM, et al. Long-term prognostic value of 13N-ammonia myocardial perfusion positron emission tomography added value of coronary flow reserve. J Am Coll Cardiol 2009;54:150–6.

[12] Dayanikli F, Grambow D, Muzik O, Mosca L, Rubenfire M, Schwaiger M. Early detection of abnormal coronary flow reserve in asymptomatic men at high risk for coronary artery disease using positron emission tomography. Circulation 1994;90:808–17.

[13] Camici PG, Crea F. Coronary microvascular dysfunction. N Engl J Med 2007;356:830–40.

[14] Reddy KG, Nair RN, Sheehan HM, Hodgson JM. Evidence that selective endothelial dysfunction may occur in the absence of angiographic or ultrasound atherosclerosis in patients with risk factors for atherosclerosis. J Am Coll Cardiol 1994;23:833–43.
[15] Kawaguchi N, Okayama H, Kawamura G, Shigematsu T, Takahashi T, Kawada Y, et al. Clinical usefulness of coronary flow reserve ratio for the detection of significant coronary artery disease on (13)N-ammonia positron emission tomography. Circ J 2018;82:486–93.
[16] Ben-Haim S, Murthy VL, Breault C, Allie R, Sitek A, Roth N, et al. Quantification of myocardial perfusion reserve using dynamic SPECT imaging in humans: a feasibility study. J Nucl Med 2013;54:873–9.
[17] Shiraishi S, Sakamoto F, Tsuda N, Yoshida M, Tomiguchi S, Utsunomiya D, et al. Prediction of left main or 3-vessel disease using myocardial perfusion reserve on dynamic thallium-201 single-photon emission computed tomography with a semiconductor gamma camera. Circ J 2015;79:623–31.
[18] Agostini D, Roule V, Nganoa C, Roth N, Baavour R, Parienti JJ, et al. First validation of myocardial flow reserve assessed by dynamic (99m)Tc-sestamibi CZT-SPECT camera: head to head comparison with (15)O-water PET and fractional flow reserve in patients with suspected coronary artery disease. The WATERDAY study. Eur J Nucl Med Mol Imaging 2018;45:1079–90.
[19] Germano G, Erel J, Lewin H, Kavanagh PB, Berman DS. Automatic quantitation of regional myocardial wall motion and thickening from gated technetium-99m sestamibi myocardial perfusion single-photon emission computed tomography. J Am Coll Cardiol 1997;30:1360–7.
[20] Klein R, Beanlands RS, deKemp RA. Quantification of myocardial blood flow and flow reserve: technical aspects. J Nucl Cardiol 2010;17:555–70.
[21] Wells RG, Timmins R, Klein R, Lockwood J, Marvin B, deKemp RA, et al. Dynamic SPECT measurement of absolute myocardial blood flow in a porcine model. J Nucl Med 2014;55:1685–91.
[22] Weich HF, Strauss HW, Pitt B. The extraction of thallium-201 by the myocardium. Circulation 1977;56:188–91.
[23] Koshino K, Fukushima K, Fukumoto M, Hori Y, Moriguchi T, Zeniya T, et al. Quantification of myocardial blood flow using (201)Tl SPECT and population-based input function. Ann Nucl Med 2014;28:917–25.
[24] ICRP. Radiation dose to patients from radiopharmaceuticals. Addendum 3 to ICRP Publication 53. ICRP Publication 106. Approved by the Commission in October 2007. Ann ICRP 2008;38:1–197.
[25] Meleca MJ, McGoron AJ, Gerson MC, Millard RW, Gabel M, Biniakiewicz D, et al. Flow versus uptake comparisons of thallium-201 with technetium-99m perfusion tracers in a canine model of myocardial ischemia. J Nucl Med 1997;38:1847–56.
[26] Ziadi MC, Dekemp RA, Williams K, Guo A, Renaud JM, Chow BJ, et al. Does quantification of myocardial flow reserve using rubidium-82 positron emission tomography facilitate detection of multivessel coronary artery disease? J Nucl Cardiol 2012;19:670–80.
[27] Fiechter M, Ghadri JR, Gebhard C, Fuchs TA, Pazhenkottil AP, Nkoulou RN, et al. Diagnostic value of 13N-ammonia myocardial perfusion PET: added value of myocardial flow reserve. J Nucl Med 2012;53:1230–4.
[28] Naya M, Murthy VL, Taqueti VR, Foster CR, Klein J, Garber M, et al. Preserved coronary flow reserve effectively excludes high-risk coronary artery disease on angiography. J Nucl Med 2014;55:248–55.
[29] Garcia EV, Faber TL, Esteves FP. Cardiac dedicated ultrafast SPECT cameras: new designs and clinical implications. J Nucl Med 2011;52:210–7.
[30] Tanaka H, Chikamori T, Tanaka N, Hida S, Igarashi Y, Yamashita J, et al. Diagnostic performance of a novel cadmium-zinc-telluride gamma camera system assessed using fractional flow reserve. Circ J 2014;78:2727–34.
[31] Garcia EV. Are SPECT measurements of myocardial blood flow and flow reserve ready for clinical use? Eur J Nucl Med Mol Imaging 2014;41:2291–3.
[32] Ben Bouallegue F, Roubille F, Lattuca B, Cung TT, Macia JC, Gervasoni R, et al. SPECT myocardial perfusion reserve in patients with multivessel coronary disease: correlation with angiographic findings and invasive fractional flow reserve measurements. J Nucl Med 2015;56:1712–7.
[33] Fukushima K, Javadi MS, Higuchi T, Bravo PE, Chien D, Lautamaki R, et al. Impaired global myocardial flow dynamics despite normal left ventricular function and regional perfusion in chronic kidney disease: a quantitative analysis of clinical 82Rb PET/CT studies. J Nucl Med 2012;53:887–93.
[34] Crawford JH, Isbell TS, Huang Z, Shiva S, Chacko BK, Schechter AN, et al. Hypoxia, red blood cells, and nitrite regulate NO-dependent hypoxic vasodilation. Blood 2006;107:566–74.
[35] Danad I, Raijmakers PG, Appelman YE, Harms HJ, de Haan S, Marques KM, et al. Quantitative relationship between coronary artery calcium score and hyperemic myocardial blood flow as assessed by hybrid 15O-water PET/CT imaging in patients evaluated for coronary artery disease. J Nucl Cardiol 2012;19:256–64.
[36] von Scholten BJ, Hasbak P, Christensen TE, Ghotbi AA, Kjaer A, Rossing P, et al. Cardiac (82)Rb PET/CT for fast and non-invasive assessment of microvascular function and structure in asymptomatic patients with type 2 diabetes. Diabetologia 2016;59:371–8.
[37] Triantafyllidi H, Pavlidis G, Trivilou P, Ikonomidis I, Tzortzis S, Xenogiannis I, et al. The association of elevated HDL levels with carotid atherosclerosis in middle-aged women with untreated essential hypertension. Angiology 2015;66:904–10.
[38] Bravo PE, Pinheiro A, Higuchi T, Rischpler C, Merrill J, Santaularia-Tomas M, et al. PET/CT assessment of symptomatic individuals with obstructive and nonobstructive hypertrophic cardiomyopathy. J Nucl Med 2012;53:407–14.
[39] Juarez-Orozco LE, Glauche J, Alexanderson E, Zeebregts CJ, Boersma HH, Glaudemans AW, et al. Myocardial perfusion reserve in spared myocardium: correlation with infarct size and left ventricular ejection fraction. Eur J Nucl Med Mol Imaging 2013;40:1148–54.
[40] Kato S, Saito N, Kirigaya H, Gyotoku D, Iinuma N, Kusakawa Y, et al. Impairment of coronary flow reserve evaluated by phase contrast cine-magnetic resonance imaging in patients with heart failure with preserved ejection fraction. J Am Heart Assoc 2016;5. pii: e002649.
[41] Sdringola S, Johnson NP, Kirkeeide RL, Cid E, Gould KL. Impact of unexpected factors on quantitative myocardial perfusion and coronary flow reserve in young, asymptomatic volunteers. JACC Cardiovasc Imaging 2011;4:402–12.